Received: 13 January 2021 | Revised: 20 February 2021 | Accepted: 6 March 2021

DOI: 10.1002/qre.2877

RESEARCH ARTICLE

WILEY

A progressive approach for the detection of the coefficient of variation

Rui Chen[1,2] | **Li Jin**[1] | **Zhonghua Li**[3] | **Jiujun Zhang**[1]

[1] Department of Mathematics, Liaoning University, Shenyang, China

[2] School of Mathematics and Statistics, Hebei University of Economics and Business, Shijiazhuang, China

[3] School of Statistics and Data Science, LPMC and KLMDASR, Nankai University, Tianjin, China

Correspondence
Jiujun Zhang, Department of Mathematics, Liaoning University, Shenyang 110036, PR China.
Email: zjjly790816@163.com

Funding information
Project of Hebei Educational Department of China, Grant/Award Numbers: 2018GJJG177, GH201007; Project of Science and Research of Liaoning Educational Department of China, Grant/Award Number: LJC202006; General Program of Natural Science Foundation of Liaoning Province, Grant/Award Number: 2020-MS-139; Science and Technology Project of Hebei Science and Technology Department of China, Grant/Award Number: 162176489; Program of Natural Science Foundation of Liaoning Province, Grant/Award Number: 2019ZD-0193; Project of Science and Research of Hebei Educational Department of China, Grant/Award Numbers: QN2017328, ZD2019073; Project of Science and Research of Hebei University of Economics and Business, Grant/Award Numbers: 2017KYQ09, 2018ZD06; National Natural Science Foundation of China, Grant/Award Number: 12071233; General Program of Natural Science Foundation of Hebei Province, Grant/Award Number: A2019207064

Abstract

A progressive average chart usually triggers initial out-of-control (OC) signals more simply and quickly than other memory-type charts . In this paper, two progressive average control procedures are proposed for monitoring the coefficient of variation (CV) of a normally distributed process variable, namely, the progressive CV (PCV) and progressive resetting CV (PRCV) control charts , respectively. The implementation of the proposed charts is presented, and the necessary design parameters are provided. Through extensive numerical simulations, it is shown that the proposed PCV and PRCV charts outperform several existing control charts to detect the initial OC signals, especially for the small and moderate CV shifts, under each combination of the shift size, the sample size, and the in-control target value of the CV. In addition, the application of the proposed control charts is illustrated by a detection example for a spinning process.

KEYWORDS

adjusted time-varying control limits, average run length, coefficient of variation, progressive average

1 | INTRODUCTION

Control charts are one of the crucial tools in statistical process control (SPC) and have been played an irreplaceable role in practice. In many processes, the mean μ and the standard deviation σ of the variable data are usually two important detection indexes, which are allowed to change within the controllable intervals of the nominal values of μ and σ. The nominal values are specified at certain constants. However, in some cases, neither the mean nor the variability is constant. They may vary subject only to the ratio γ of the standard deviation to the mean, so that γ named as the coefficient of

variation (CV) is constant. Especially, for comparing the variability among several variable groups without the same unit of measurement or the mean, the CV is applied more meaningfully and widely than the standard deviation. The CV is the relative variation, which is a dimensionless measure.

Kang et al[1] proposed the first Shewhart-type CV control chart of a normally distributed process. Similar to any Shewhart-type scheme, it is sensitive to large shifts. To enhance the monitoring capability of the CV scheme, an exponentially weighted moving average (EWMA) CV procedure was designed by Hong et al.[2] Based on the average run length (ARL), which is one of the most common measures of control chart performance, the results clearly showed that this scheme[2] outperforms the above scheme.[1] Subsequently, Castagliola et al[3] developed two one-sided EWMA (OSE) charts for monitoring the CV squared instead of the CV. That is more sensitive than the previous method.[2] Later, a synthetic CV control chart was suggested by Calzada and Scariano,[4] which is better than the Shewhart scheme[1] but weaker than the OSE method. An adaptive Shewhart procedure was proposed by Castagliola et al,[5] which implements a variable sampling interval strategy. Castagliola et al[6] developed a Shewhart model with supplementary run rules. However, the performances of these Shewhart-type charts are still no more sensitive than those of the OSE method.

To enhance the sensitivity of the OSE method, based on the preliminary work,[3] new modified OSE (MOSE) charts were developed by Zhang et al.[7] It was shown the MOSE schemes have ARL performances superior to those of the competing schemes by many comparisons. Castagliola et al[8] developed Shewhart-type charts based on short production runs. Amdouni et al[9] proposed a variable sample size model using the continuously variable sampling scheme suggested by Li and Qiu.[10] Besides, You et al[11] suggested a side sensitive group runs procedure. Zhang et al[12] designed a resetting EWMA (RES) scheme, which resets the normalized observations to the target in the traditional EWMA statistics. Chen et al[13] proposed the generally weighted moving average (GWMA) charts for monitoring the process CV, which incorporates a one-sided resetting model in a GMWA (OSRG) scheme to improve the performance of the CV control scheme. Abbasi et al[14] designed the CV charts based on ranked set sampling, which are better than the classical CV scheme under simple random sampling chart in terms of the run length (RL) performance. Abbasi[15] proposed the CV chart by using auxiliary information based on ratio, regression, and hybrid estimators for efficient detection of the process CV.

The goal of this paper is to further enhance the sensitivity of the CV schemes. To this end, this paper proposes a progressive approach which is a memory-type control structure. First, Agarwal[16] (2003, p. 38) defined progressive mean (PM) as follows. "In progressive average, we find out the average of first two periods value and then go on adding the value for third, fourth, fifth period, etc., and calculate the averages of three, four, five, etc., period successively. Such averages are called progressive average." Abbas et al[17] proposed an effective PM control scheme to detect the small and moderate shifts of the process location parameter. Abbasi et al[18] suggested a nonparametric PM chart for monitoring the process target or location. It was shown that this scheme is more sensitive than the other nonparametric schemes. Zafar et al[19] designed the progressive variance structure. Abbas[20] expounded the PM model, in which the smoothing parameter is updated after every sample, is a special type of the EWMA model. Based on Poisson distribution, Abbasi[21] proposed a PM scheme, which has a greater ability for monitoring the out-of-control (OC) signals. Zafar et al[22] suggested the PM procedure for joint detection of the dispersion and location. To enhance the sensitivity of the PM scheme, Abbas et al[23] designed the double PM and optimal double PM models. Alevizakos and Koukouvinos[24] showed a PM scheme for detection of the time between events.

In this paper, the progressive CV control model is proposed, which is abbreviated as the PCV chart. In addition, we combine the PM procedure with a resetting model, referred to as the PRCV chart. The resetting technique was originally suggested by Shu and Jiang,[25] which can overcome the inertia of memory-type schemes and enhance the sensitivity of the control model.

The rest of this paper is as follows. The proposed PCV and PRCV charts are introduced in Section 2. Section 3 investigates the implementation issues related to the proposed schemes and compares the performances of the PCV and PRCV methods. In terms of the ARL, the proposed schemes are compared with several other powerful CV schemes in Section 4. Section 5 presents an illustrative example from a spinning process. Some concluding remarks with comments are summarized in Section 6.

2 | THE PROPOSED PROGRESSIVE CV SCHEMES

2.1 | The structure of the PM model

To help to better understand how the proposed PCV and PRCV control charts are developed, the PM control chart is briefly introduced herein. Suppose the observations $\{X_k\}(k = 1, 2, ...)$ are the quality characteristics to be monitored. They

are assumed to obey an identically independent normal distribution with a mean of the process μ_0 and standard deviation σ_0. The PM statistic is a cumulative average, which is defined as

$$PM_k = \frac{\sum_{i=1}^{k} X_i}{k}. \tag{1}$$

Then $\mu_{PM_k} = \mu_0$ and $\sigma_{PM_k} = \frac{\sigma_0}{\sqrt{k}}$. So the $3-\sigma$ limits are obtained as follows:

$$\begin{aligned} UCL_k &= \mu_0 + 3 \cdot \frac{\sigma_0}{\sqrt{k}}, \\ CL_k &= \mu_0, \\ LCL_k &= \mu_0 - 3 \cdot \frac{\sigma_0}{\sqrt{k}}. \end{aligned} \tag{2}$$

Abbas et al[17] discussed that the control limits remain too wide for the larger values of k, as a result, the scheme fails to signal for the OC sample. To make the limits narrower for the later samples, a simple function of k ($f(k) = k^{0.2}$ usually adopted) is put into the limits, as follows:

$$\begin{aligned} UCL_k &= \mu_0 + 3 \cdot \frac{\sigma_0}{\sqrt{k}}\left(\frac{L}{f(k)}\right), \\ CL_k &= \mu_0, \\ LCL_k &= \mu_0 - 3 \cdot \frac{\sigma_0}{\sqrt{k}}\left(\frac{L}{f(k)}\right), \end{aligned} \tag{3}$$

where L is a constant of the control limit.

Based on the progressive statistics (see Agarwal[16] and Abbas et al[17] for more details), we propose two progressive CV schemes for monitoring the process CVs, named as the PCV and PRCV charts.

2.2 | The model of the PCV chart

We assume that $X_k = \{X_{k1}, X_{k2}, \ldots, X_{kn}\}$ is a collected sample of size n at times $k = 1, 2, \ldots$, which are independently and identically distributed variables, following a normal distribution $N(\mu_k, \sigma_k)$. When the process is in control (IC), the standard deviation σ_k, and the mean μ_k are constrained by $\gamma_k = \frac{\sigma_k}{\mu_k} = \gamma_0$. So the values of σ_k and μ_k may vary, but the value $\gamma_k = \frac{\sigma_k}{\mu_k}$ may be the specified IC CV value γ_0, which is a constant.

Now, $\bar{X}_k = \frac{1}{n}\sum_{i=1}^{n} X_{ki}$ and $S_k = \sqrt{\frac{1}{n-1}\sum_{i=1}^{n}(X_{ki} - \bar{X}_k)^2}$ are the sample mean of X_k and the sample standard deviation, respectively. Then the sample CV of X_k is $\hat{\gamma}_k = \frac{S_k}{\bar{X}_k}$. The distributional properties of $\hat{\gamma}$ have been proposed in the literature. Iglewicz et al[26] noted that when the population distribution is normal, $\frac{\sqrt{n}}{\hat{\gamma}_k}$ follows a t-distribution with noncentrality parameter $\frac{\sqrt{n}}{\gamma_0}$ and degrees of freedom $n-1$. In the CV control scheme, it has been proven that monitoring $\hat{\gamma}^2$ is more efficient than $\hat{\gamma}$ in the paper.[3] So the PCV scheme is based on $\hat{\gamma}^2$.

First, we define the standardized ${\hat{\gamma}_k}^2$ as

$$Z_k = \frac{{\hat{\gamma}_k}^2 - \mu_0(\hat{\gamma}^2)}{\sigma_0(\hat{\gamma}^2)}. \tag{4}$$

Here, approximations for $\mu_0(\hat{\gamma}^2)$ and $\sigma_0(\hat{\gamma}^2)$ are provided by Breunig[27] as

$$\mu_0(\hat{\gamma}^2) = \gamma_0^2\left(1 - \frac{3\gamma_0^2}{n}\right), \tag{5}$$

and

$$\sigma_0(\hat{\gamma}^2) = \left(\gamma_0^4\left(\frac{2}{n-1} + \gamma_0^2\left(\frac{4}{n} + \frac{20}{n(n-1)} + \frac{75\gamma_0^2}{n^2}\right)\right) - \left(\mu_0(\hat{\gamma}^2) - \gamma_0^2\right)^2\right)^{\frac{1}{2}}. \tag{6}$$

Therefore, Z_k approximately follows a standard normal distribution. The proposed procedure puts the standardized data Z_k into conventional progressive statistics. The plotting statistics of the upper-sided PCV chart are defined as

$$V_k^+ = \frac{\sum_{i=1}^k Z_i}{k}, \qquad k = 1, 2, \ldots. \tag{7}$$

The asymptotic IC values of $\mu(V_k^+)$ and $\sigma^2(V_k^+)$ are calculated as

$$\mu(V_k^+) = 0$$

and

$$\sigma^2(V_k^+) = \frac{1}{k}.$$

Finally, the time-varying upper-sided control limits (UCL) can be calculated as follows:

$$UCL_k = L^+ \cdot \frac{1}{f(k)}\sqrt{\frac{1}{k}}, \qquad k = 1, 2, \ldots, \tag{8}$$

where L^+ is charting constant obtained via the following bisection searching algorithms. In this paper, we use $f(k) = k^{0.2}$. When $V_k^+ > UCL_k$, an alarm is triggered.

Analogously, the lower-sided PCV statistics are defined as

$$V_k^- = \frac{\sum_{i=1}^k Z_i}{k}, \qquad k = 1, 2, \ldots. \tag{9}$$

It can be obtained that $\mu(V_k^-) = 0$ and $\sigma^2(V_k^-) = \sigma^2(V_k^+) = \frac{1}{k}$ are the asymptotic values of mean and variance of Equation (9), respectively. Hence, the corresponding lower-sided control limits (LCL) are

$$LCL_k = -L^- \cdot \frac{1}{f(k)}\sqrt{\frac{1}{k}}, \qquad k = 1, 2, \ldots, \tag{10}$$

where L^- is the charting constant of the downward PCV scheme. When $V_k^- < LCL_k$, an alarm is triggered.

2.3 | The model of the PRCV chart

We incorporate a resetting feature in the PCV procedure so that the sensitivity of the CV schemes may be further improved. Now, Equation (7) can be revised as

$$U_k^+ = \frac{\sum_{i=1}^k Z_i^+}{k}, \qquad k = 1, 2, \ldots \tag{11}$$

where $Z_i^+ = \max(0, Z_i)$.

In the case of $Z_i \sim N(0, 1)$, the numerical characteristic of Z_i^+, is given by Barr and Sherrill.[28]

$$\mu(Z_i^+) = \frac{1}{\sqrt{2\pi}}, \qquad \sigma^2(Z_i^+) = \frac{1}{2} - \frac{1}{2\pi}.$$

Hence, the control limits in the upward PRCV chart are

$$UCL_k = \frac{1}{\sqrt{2\pi}} + L^+ \cdot \frac{1}{f(k)} \sqrt{\left(\frac{1}{2} - \frac{1}{2\pi}\right)\frac{1}{k}}, \qquad k = 1, 2, \ldots. \tag{12}$$

In the same way, the downward PRCV control chart is

$$U_k^- = \frac{\sum_{i=1}^{k} Z_i^-}{k}, \qquad k = 1, 2, \ldots, \tag{13}$$

where $Z_i^- = \min(0, Z_i)$.

The corresponding downward control limits are

$$LCL_k = \frac{1}{\sqrt{2\pi}} - L^- \cdot \frac{1}{f(k)} \sqrt{\left(\frac{1}{2} - \frac{1}{2\pi}\right)\frac{1}{k}}, \qquad k = 1, 2, \ldots. \tag{14}$$

In the upward and downward PRCV charts, the $f(k)$ of the control limits is identified as $k^{0.2}$.

3 | IMPLEMENTATION ISSUES

First of all, to identify the charting constants, we provide a search algorithm based on a Monte Carlo simulation and bisection method. Then, we discuss the performance of the proposed schemes.

The RL is defined as the number of samples collected from the initial time point to the occurrence of a false OC signal. The expectation of the RL when the process is in control is called the IC ARL (ARL_0). To avoid false alarms, the ARL_0 value should be sufficiently large in an ideal situation, which is usually fixed at a given level. The average RL collected from the occurrence of a shift to the time of the signal is called OC ARL (ARL_1). For a given control chart, the smaller its ARL_1 value is, the more quickly detects shifts.

Table 1 The control limit constant L^+ and L^- of the PCV control charts when $ARL_0 = 370$

	L^+		L^-	
n	$\gamma_0 = 0.1$	$\gamma_0 = 0.2$	$\gamma_0 = 0.1$	$\gamma_0 = 0.2$
5	1.530	4.370	0.330	−0.38
10	1.330	3.490	0.375	−0.264
15	1.200	3.000	0.433	−0.18
20	1.130	2.750	0.453	−0.120
30	1.070	2.380	0.520	−0.036
50	1.000	1.970	0.560	0.100
70	0.931	1.761	0.600	0.140
100	0.90	1.601	0.603	0.230

Table 2 The control limit constant L^+ and L^- of the PRCV control charts when $ARL_0 = 370$

	L^+		L^-	
n	$\gamma_0 = 0.1$	$\gamma_0 = 0.2$	$\gamma_0 = 0.1$	$\gamma_0 = 0.2$
5	−0.080	1.050	−0.450	−0.683
10	0.400	1.700	−0.200	−0.640
15	0.610	1.750	−0.090	−0.530
20	0.690	1.760	−0.019	−0.460

Table 3 The ARL values of the upward PCV and PRCV control charts when γ_0 =0.1, 0.2, $ARL_0 = 370$, and $n = 5, 10, 15$

		$n = 5$		$n = 10$		$n = 15$	
γ_0	τ	PCV	PRCV	PCV	PRCV	PCV	PRCV
0.1	1.00	369.79	370.52	370.55	369.84	369.27	370.65
	1.01	123.43	82.51	80.73	51.64	57.26	47.94
	1.02	68.54	28.61	40.89	24.61	28.41	21.33
	1.03	47.27	17.87	26.29	15.28	18.60	13.45
	1.04	35.19	12.53	19.13	10.95	13.52	10.16
	1.05	27.56	10.08	14.91	8.73	10.49	7.98
	1.10	12.55	5.07	6.88	4.33	4.84	3.88
	1.20	5.74	2.81	3.23	2.26	2.39	1.97
	1.40	2.81	1.73	1.71	1.40	1.37	1.24
	1.60	1.96	1.40	1.31	1.16	1.13	1.08
	1.80	1.59	1.24	1.15	1.07	1.05	1.03
	2.00	1.40	1.14	1.07	1.04	1.01	1.01
		$n = 5$		$n = 10$		$n = 15$	
γ_0	τ	PCV	PRCV	PCV	PRCV	PCV	PRCV
0.2	1.00	369.17	370.69	370.91	371.01	369.98	370.34
	1.01	226.46	103.39	167.04	90.78	128.39	80.73
	1.02	158.27	55.08	101.58	49.71	71.27	41.70
	1.03	119.68	36.45	69.88	32.96	48.29	26.92
	1.04	93.72	26.49	51.97	23.26	34.78	19.33
	1.05	76.74	20.91	41.15	18.49	27.25	14.91
	1.10	36.99	10.01	18.23	8.23	11.90	6.55
	1.20	15.84	4.69	7.68	3.64	5.00	2.90
	1.40	6.52	2.42	3.26	1.84	2.25	1.50
	1.60	3.92	1.78	2.08	1.37	1.52	1.18
	1.80	2.82	1.47	1.59	1.18	1.24	1.07
	2.00	2.24	1.30	1.35	1.11	1.12	1.04

3.1 | Search algorithm

Based on the bisection method (see Chen et al,[13] Qiu,[29] and Li et al[30]) and a Monte Carlo simulation, the search algorithm for the charting constants L^+ and L^- is used. The bisection method is an iterative algorithm. Based on monotonicity, comparing the values of intermediate nodes achieves the purpose of narrowing the range to searched elements. That is the essence of bisection.

Tables 1 and 2 present the L^+ and L^- values of the PCV and PRCV schemes for different combinations of (γ_0, n) when ARL_0 is 370. In Tables 1 and 2, all results were implemented in Fortran 90 with the IMSL package. To balance time consumption and accuracy, we recommend the maximum of 10,000 iterations.

It is presented that the charting constant L^+ or L^- is affected by the parameters γ_0 and n in Tables 1 and 2. For any fixed (n, γ_0), as n increases, the L^+ values decrease and the L^- values increase in the PCV control charts. However, the L^+ and L^- values all increase in the PRCV control charts when n increases. For any fixed n, as γ_0 increases, L^+ increases, and L^- decreases in both PCV and PRCV charts. In general, for any fixed (n, γ_0), L^+ and L^- show uniform trends of variation in the PCV and PRCV charts, respectively.

3.2 | Performance analysis

Utilizing simulation, we obtain the value of the zero-state ARL_1, which provides a reference for monitoring capability of the CV scheme. First, jointly select the n and L values that yield a target zero-state ARL_0 when the process is in control,

Table 4 The ARL values of the downward PCV and PRCV control charts when γ_0 =0.1, 0.2, $ARL_0 = 370$, and $n = 5, 10, 15$

		$n = 5$		$n = 10$		$n = 15$	
γ_0	τ	PCV	PRCV	PCV	PRCV	PCV	PRCV
0.1	1.00	370.84	369.71	369.77	369.83	370.10	370.41
	0.99	81.50	270.97	39.08	75.51	30.75	35.43
	0.98	24.39	142.64	15.45	16.66	12.54	12.86
	0.97	13.49	41.76	9.59	8.80	7.83	7.55
	0.96	9.91	11.85	6.77	5.97	5.84	5.24
	0.95	7.38	5.99	5.27	4.71	4.56	4.26
	0.90	3.47	2.62	2.59	2.38	2.26	2.17
	0.80	1.77	1.51	1.42	1.36	1.29	1.25
	0.60	1.09	1.05	1.02	1.01	1.00	1.00
	0.40	1.00	1.00	1.00	1.00	1.00	1.00
	0.20	1.00	1.00	1.00	1.00	1.00	1.00
		$n = 5$		$n = 10$		$n = 15$	
γ_0	τ	PCV	PRCV	PCV	PRCV	PCV	PRCV
0.2	1.00	369.17	370.53	370.84	370.87	370.18	370.56
	0.99	211.63	278.32	90.59	204.02	34.17	123.20
	0.98	75.47	101.83	11.41	63.32	7.69	11.81
	0.97	14.57	23.05	5.54	9.76	4.36	5.53
	0.96	6.35	7.31	3.63	4.47	3.32	3.74
	0.95	4.27	4.69	2.97	3.25	2.61	2.96
	0.90	1.93	2.76	1.61	1.79	1.51	1.68
	0.80	1.22	1.39	1.13	1.20	1.08	1.14
	0.60	1.01	1.03	1.00	1.00	1.00	1.00
	0.40	1.00	1.00	1.00	1.00	1.00	1.00
	0.20	1.00	1.00	1.00	1.00	1.00	1.00

$\gamma = \gamma_0$. Then,

$$ARL_1 = ARL(\gamma_1, \gamma_0, L, n) \tag{15}$$

subject to the constraint

$$ARL(\gamma_0, \gamma_0, L, n) = ARL_0. \tag{16}$$

That is, based on the charting constant L selected above, the procedure yields the zero-state ARL_1 for a specified $\gamma = \gamma_1 = \tau\gamma_0 \neq \gamma_0$, where $0 < \tau < 1$ corresponds to a downward shift in the nominal CV, while $\tau > 1$ corresponds to an upward CV shift.

Based on the algorithm above, when the ARL_0 value is prespecified as 370, and the different levels of the parameters (i.e., $\gamma_0 = 0.1$ or 0.2; $n = 5$, 10, or 15) are chosen, the ARL_1 values are presented in Tables 3 and 4, which provide the OC performance characteristics of the PCV and PRCV schemes. From Tables 3 and 4, we can find that the values of ARL_1 are influenced by the two parameters n and γ_0.

We analyze the influences of parameters on the ARL. First, the ARL_1 values are compared under different values of γ_0. We find the values of ARL_1 are generally larger in the upward PCV and PRCV schemes when $\gamma_0 = 0.2$ than those of $\gamma_0 = 0.1$. This conclusion also applies to the downward PCV and PRCV schemes when $0.98 \leq \tau < 1$, while the reverse is true when $\tau < 0.98$. In addition, ARL_1 decreases as n increases in PCV and PRCV charts for monitoring any upward or downward CV shift. Considering the effect of n, a larger value of n can improve the sensitivity of the scheme.

Table 5 The effect on the IC ARL values of the upward PCV and PRCV control charts when the CV varies within −5% to +5% ($ARL_0 = 370$)

		$n = 5$		$n = 10$		$n = 15$	
γ_0	Actual γ_0	PCV	PRCV	PCV	PRCV	PCV	PRCV
0.1	0.095	407.31	400.51	401.31	390.67	400.33	400.01
	0.096	395.84	377.70	399.86	379.88	399.56	393.99
	0.097	387.38	375.03	389.15	374.80	387.03	398.55
	0.098	383.67	373.88	383.30	371.87	373.32	389.69
	0.099	378.00	372.39	379.43	369.70	371.11	381.53
	0.100	369.79	370.52	370.55	369.84	369.07	370.65
	0.101	362.11	369.12	368.84	357.69	368.01	368.39
	0.102	349.31	361.20	367.08	361.79	358.07	362.61
	0.103	345.66	372.26	362.00	351.83	352.65	360.28
	0.104	344.00	365.54	360.33	347.55	351.01	365.03
	0.105	340.10	336.18	346.61	340.89	349.91	351.87
		$n = 5$		$n = 10$		$n = 15$	
γ_0	Actual γ_0	PCV	PRCV	PCV	PRCV	PCV	PRCV
0.2	0.190	413.43	430.83	420.45	420.57	418.79	421.69
	0.192	402.99	411.58	412.06	414.49	410.86	405.85
	0.194	394.56	403.58	399.08	398.95	396.60	394.32
	0.196	383.46	382.05	393.83	388.81	381.09	375.21
	0.198	378.48	378.05	384.46	373.68	373.83	373.21
	0.200	369.17	370.69	370.91	371.01	369.98	370.34
	0.202	363.70	353.96	364.92	366.98	357.31	351.42
	0.204	350.61	345.53	351.29	344.97	350.63	352.83
	0.206	337.85	332.85	345.34	342.08	343.45	340.30
	0.208	333.58	317.71	338.75	333.91	335.59	330.00
	0.210	327.07	316.84	327.98	326.01	331.66	316.13

Next, the performances of the PCV scheme are compared with the PRCV scheme for the same parameters. In Table 3, the performances of the PRCV chart are better than those of the PCV chart for detection of the small or moderate upward shifts. Moreover, the smaller the magnitude of the upward shift is, the more significant the sensitivity of the PRCV chart is than that of the PCV chart. For instant, for $\gamma_0 = 0.1$, $n = 5$, and $\tau = 1.05$, the ARL_1 value of the PRCV scheme is 10.08, which is 63.43% less than the value of 27.56 for the PCV scheme. The ARL_1 of the PRCV chart is 2.81, which is 51.05% less than the value of 5.74 for the PCV chart when $\gamma_0 = 0.1$, $n = 5$, and $\tau = 1.20$. However, with the increase of n, the advantage of the PRCV scheme gradually decreases compared with the PCV scheme for the upward shifts. To detect large upward shifts, the sensitivity of the two schemes is similar, although the PRCV chart is slightly better than the PCV chart.

We analyze the sensitivity of the downward PCV and PRCV charts from Table 4. When $\gamma = 0.2$, the performance of the PCV scheme is more sensitive than that of the PRCV scheme for monitoring the downward shifts of various magnitudes. For $\gamma = 0.1$, when $0.95 < \tau < 1$, the sensitivity of the PCV scheme is better than that of the PRCV scheme, but when $\tau \leq 0.95$, the sensitivity of the PRCV scheme is slightly better than that of the PCV scheme. Thus, the advantage of the PCV scheme is more significant than that of the PRCV scheme for the small downward shifts ($0.95 < \tau < 1$), while the sensitivities of the PCV and PRCV schemes are similar for the medium and large downward shifts.

In general, the sensitivities of the PCV and PRCV charts are predominantly influenced by n. To rapidly detect any upward or downward CV shift, a practitioner can choose n as large as possible. For monitoring the upward CV shifts, we may choose the PRCV scheme with better performances, while for detection of the downward CV shifts, the PCV scheme is an ideal choice.

Table 6 The effect on the IC ARL values of the downward PCV and PRCV control charts when the CV varies within −5% to +5% ($ARL_0 = 370$)

		$n = 5$		$n = 10$		$n = 15$	
γ_0	Actual γ_0	PCV	PRCV	PCV	PRCV	PCV	PRCV
0.1	0.095	351.94	368.67	343.72	362.01	351.79	362.80
	0.096	352.64	367.66	350.15	366.89	353.12	364.89
	0.097	360.78	369.29	352.11	365.43	353.98	360.84
	0.098	366.77	372.38	353.76	371.23	366.62	361.78
	0.099	369.57	375.07	370.98	375.92	371.15	351.89
	0.100	370.84	369.71	369.77	369.83	370.10	370.41
	0.101	378.51	398.86	380.51	391.58	373.68	373.73
	0.102	394.20	396.48	383.79	392.06	383.06	375.06
	0.103	383.78	400.34	377.36	393.98	376.50	400.07
	0.104	406.63	413.33	375.86	409.98	384.22	403.09
	0.105	412.72	415.12	383.10	410.73	385.01	378.82
		$n = 5$		$n = 10$		$n = 15$	
γ_0	Actual γ_0	PCV	PRCV	PCV	PRCV	PCV	PRCV
0.2	0.190	333.07	350.96	329.77	352.70	332.90	349.47
	0.192	334.06	351.37	353.08	360.69	355.45	350.02
	0.194	336.40	363.81	352.30	359.17	345.31	356.77
	0.196	350.13	360.22	351.42	358.09	348.57	363.11
	0.198	357.99	361.01	368.99	355.88	349.72	368.97
	0.200	369.17	370.53	370.84	370.87	370.18	370.56
	0.202	382.56	378.23	372.27	379.56	377.64	380.85
	0.204	403.22	385.83	387.00	391.01	394.34	390.95
	0.206	404.24	390.31	394.05	389.17	387.22	396.13
	0.208	405.45	395.08	395.11	404.31	400.76	401.91
	0.210	401.37	400.30	400.43	400.94	403.57	403.83

3.3 | Robustness analysis

3.3.1 | The effect of the CV variation on the performance of the proposed approaches

In practice, the value of γ_0 is usually unknown and has to be estimated. We might as well assume that the actual value of CV fluctuates within −5 to +5% of the given nominal value γ_0. In this case, the effects on the IC performances of the control charts are shown in Tables 5 and 6. From Table 5, we obtain that it is slightly more affected by the variation of the CV values when given $\gamma_0 = 0.2$ than $\gamma_0 = 0.1$ in the upward PCV and PRCV control charts. The actual values of the ARL_0 vary within −14% to +15% when the CV varies within −5% to +5%, which are acceptable. From Table 6, it is shown that the effects of the CV variation on the values of IC ARL of the downward PCV and PRCV control charts are similar. The actual values of the ARL_0 vary within −11% to +12%, which are also acceptable. So when the CV varies within −5% to +5%, it will affect the IC performance of the PCV and PRCV control charts in an acceptable range.

The effects of the CV variation at ±5% on the OC performances of the PCV and PRCV charts are tabulated in the case of the nominal CV value $\gamma_0 = 0.2$ and $n = 10$ (that is, the actual CV value $\gamma_0 = 0.21$ and $\gamma_0 = 0.19$, respectively). From Tables 7 and 8, it is shown that the values of ARL_1 when the actual CV value is 0.19 or 0.21 are very close to the value of ARL_1 corresponding to the nominal value of $\gamma_0 = 0.2$. Hence, the OC performances of the proposed charts are very little affected by the variation of the CV value.

Table 7 The effect on the OC ARL and SDRL values of the upward PCV and PRCV control charts when the CV varies ($ARL_0 = 370$, γ_0 =0.2, and $n = 10$)

	PCV						PRCV					
	$\gamma_0 = 0.2$		$\gamma_0 = 0.19$		$\gamma_0 = 0.21$		$\gamma_0 = 0.2$		$\gamma_0 = 0.19$		$\gamma_0 = 0.21$	
τ	ARL	SDRL	ARL	SDRL	ARL	SDRL	ARL	SDRL	ARL	SDRL	ARL	SDRL
1.01	226.46	198.10	176.88	211.73	155.14	180.49	95.07	223.21	97.78	235.79	90.57	208.17
1.02	158.27	106.91	104.72	112.50	96.82	100.58	48.99	95.18	51.28	100.66	47.52	91.91
1.03	119.68	68.82	71.78	71.32	67.21	65.98	33.14	57.87	32.95	57.12	32.21	56.66
1.04	93.72	48.12	54.09	50.98	51.33	47.55	23.63	37.67	23.77	38.14	23.59	37.31
1.05	76.74	36.51	41.51	37.34	40.50	35.86	18.64	27.82	18.73	28.12	18.30	27.24
1.10	36.99	14.45	18.37	14.51	18.26	14.41	8.29	10.09	8.18	9.97	8.18	9.86
1.15	23.04	8.21	11.11	8.28	10.99	8.11	5.12	5.44	5.12	5.43	5.13	5.44
1.20	15.84	5.45	7.71	5.45	7.69	5.46	3.68	3.57	3.66	3.55	3.70	3.56
1.30	9.48	3.10	4.61	3.07	4.60	3.07	2.40	1.97	2.38	1.94	2.41	1.99
1.40	6.52	2.07	3.24	2.07	3.26	2.10	1.81	1.27	1.83	1.29	1.83	1.29
1.50	4.91	1.54	2.51	1.53	2.53	1.54	1.53	0.93	1.53	0.91	1.56	0.95

Table 8 The effect on the OC ARL and SDRL values of the downward PCV and PRCV control charts when the CV varies ($ARL_0 = 370$, γ_0 =0.2, and $n = 10$)

	PCV						PRCV					
	$\gamma_0 = 0.2$		$\gamma_0 = 0.19$		$\gamma_0 = 0.21$		$\gamma_0 = 0.2$		$\gamma_0 = 0.19$		$\gamma_0 = 0.21$	
τ	ARL	SDRL	ARL	SDRL	ARL	SDRL	ARL	SDRL	ARL	SDRL	ARL	SDRL
0.99	90.59	841.66	63.13	652.74	112.53	972.46	204.02	1474.65	161.95	1233.90	232.12	1487.40
0.98	11.41	93.58	10.25	80.35	12.90	107.18	63.32	797.11	49.76	615.80	92.93	909.02
0.97	5.54	26.97	5.13	23.66	5.79	30.09	9.76	167.44	7.92	78.86	11.02	179.92
0.96	3.63	13.67	3.49	11.08	3.77	13.91	4.47	29.30	4.67	30.39	5.26	38.34
0.95	2.90	9.16	2.86	8.41	3.11	9.26	3.25	15.40	3.27	13.06	3.57	17.06
0.90	1.60	2.25	1.61	2.23	1.63	2.24	1.79	2.60	1.78	2.50	1.82	2.82
0.85	1.27	1.00	1.26	0.95	1.27	0.99	1.35	1.15	1.38	1.14	1.40	1.20
0.80	1.13	0.51	1.12	0.53	1.13	0.54	1.20	0.62	1.20	0.67	1.20	0.63
0.65	1.01	0.08	1.01	0.08	1.01	0.08	1.02	0.13	1.02	0.14	1.02	0.14

3.3.2 | The effect of estimated parameters on the performance of the proposed approaches

When the IC CV value γ_0 is unknown, it need be estimated from the samples taken when the process is in control. This stage in control process is called Phase I. It is known that the estimated CV of the quality characteristic X is usually defined as sample CV of X_k, $\widehat{\gamma_k} = \frac{S_k}{\overline{X}_k}$. In the case of multiple samples, the commonly used CV estimation is the mean of the sample CV and is defined as

$$\bar{\hat{\gamma}} = \frac{1}{m}\sum_{k=1}^{m}\frac{S_k}{\overline{X}_k}. \tag{17}$$

In the paper, we adopt Equation (17) as the estimator of CV based on m samples of size n in Phase I.

Now, the effect of parameter estimation on the performance of the proposed control charts is analyzed. The simulation process is as follows.

(1) First, suppose the parameter γ_0 is known. Through 20,000 simulation runs, the control limit of the proposed chart is calculated. The simulation results of control limit constants L^+ and L^- are shown in Tables 1 and 2 for the different values of the combination (γ_0, n) when the controlled ARL reach to 370.

Table 9 ARL_1 values of the PCV, PRCV, OSRG ($q = 0.95, \alpha = 0.75$), RES, MOSE, and OSE charts ($ARL_0 = 370$)

		$n = 5$						$n = 10$					
γ_0	τ	PCV	PRCV	OSRG	RES	MOSE	OSE	PCV	PRCV	OSRG	RES	MOSE	OSE
0.1	0.50	1.0	1.0	2.6	4.1	4.5	4.8	1.0	1.0	1.8	2.3	2.4	2.5
	0.65	1.2	1.1	4.5	7.5	7.9	8.8	1.1	1.0	2.9	4.1	4.3	4.6
	0.80	1.8	1.5	11.4	17.6	17.6	20.6	1.4	1.4	7.0	10.2	10.1	11.4
	0.90	3.5	2.6	34.8	51.3	43.4	54.1	2.6	2.4	21.0	29.3	25.6	30.9
	1.10	12.6	5.1	35.9	46.5	44.5	51.5	6.9	4.3	21.0	27.9	26.5	30.4
	1.25	4.6	2.4	9.4	13.6	13.7	15.2	2.6	1.9	5.1	7.9	7.8	8.5
	1.50	2.3	1.5	3.5	5.4	5.4	5.8	1.5	1.2	2.0	3.0	3.1	3.2
	2.00	1.4	1.1	1.7	2.3	2.3	2.4	1.1	1.0	1.1	1.4	1.4	1.4
	RMI	0.5	0.0	4.3	6.9	6.5	7.7	0.2	0.0	2.6	4.1	3.9	4.5
0.2	0.50	1.0	1.0	1.6	3.7	4.4	4.8	1.0	1.0	1.4	2.3	2.4	2.5
	0.65	1.0	1.1	2.8	6.7	8.0	8.8	1.0	1.0	2.4	4.1	4.4	4.7
	0.80	1.2	1.4	7.2	15.0	16.3	20.9	1.1	1.2	5.8	9.5	10.0	11.6
	0.90	1.9	2.8	23.1	47.5	41.1	55.4	1.6	1.8	18.0	28.0	24.8	31.7
	1.10	37.0	10.0	40.1	49.4	48.5	52.4	18.2	8.2	22.7	29.6	28.7	31.4
	1.25	12.0	3.7	10.5	14.6	14.8	15.9	5.8	2.9	5.6	8.4	8.4	4.9
	1.50	4.9	2.0	3.8	5.7	5.8	6.1	2.5	1.5	2.2	3.2	3.3	3.4
	2.00	2.2	1.3	1.8	2.4	2.5	2.6	1.4	1.1	1.2	1.5	1.5	1.5
	RMI	0.9	0.2	3.0	6.7	6.7	8.3	0.4	0.0	2.4	4.3	4.2	4.8

(2) Then, generate m random numbers of size n from a normal distribution subject only to the IC CV value of γ_0. Next based on the random numbers, calculate the estimated value of CV, $\bar{\hat{\gamma}}_j$ in Equation (17). The value of $\bar{\hat{\gamma}}_j$ is used to replace the value of the parameter γ_0 in Equations (5) and (6).

(3) The proposed control chart statistics are calculated using the estimated parameters in Step (2) based on the randomly generated sample of size n, X_{k_i}. Then this k_ith obtained values of the statistics are compared with the corresponding the control limits obtained in Step (1).

(4) Step (3) is repeated until an alarm is triggered, then we record the value of RL_k. Here, the maximum number of the times of repeat is set to 10,000, that is, $i \leq 10,000$.

(5) Steps (3) and (4) are repeated 10,000 times, then the value of ARL_j is calculated as follow

$$ARL_j = \frac{1}{10,000} \sum_{k=1}^{10,000} RL_k.$$

(6) Steps (2)–(5) are repeated 500 times, then the average ARL (AARL) is calculated as follow :

$$AARL = \frac{1}{500} \sum_{j=1}^{500} ARL_j.$$

By extensive simulation results, we find that if the number of the samples m increases, the estimator of CV $\bar{\hat{\gamma}}$ will gradually decrease from greater than the true value γ_0 to less than γ_0 and finally approach and stabilize to γ_0. This leads to the decrease of the mean μ and variance σ of the corresponding statistic (see Equations 5 and 6) when the decrease of the estimator of CV in the control charts (i.e., when the increase of m). Hence, when the upward control limit UCL remains invariant, the value of the standardized statistic increases from $V_k^+ < UCL$ to close to UCL when the estimator of CV $\bar{\hat{\gamma}}$ decreases. This results in a decrease in the value of IC ARL of the upward proposed chart from $ARL_0 > 370$ to slowly approaching 370 (the desired ARL_0 value is 370) when the number of samples m increases.

Thus, it is shown that the IC performance of the proposed upward charts is less affected when the IC CV values are estimated using a small number of Phase-I samples, m, in terms of the IC ARL.

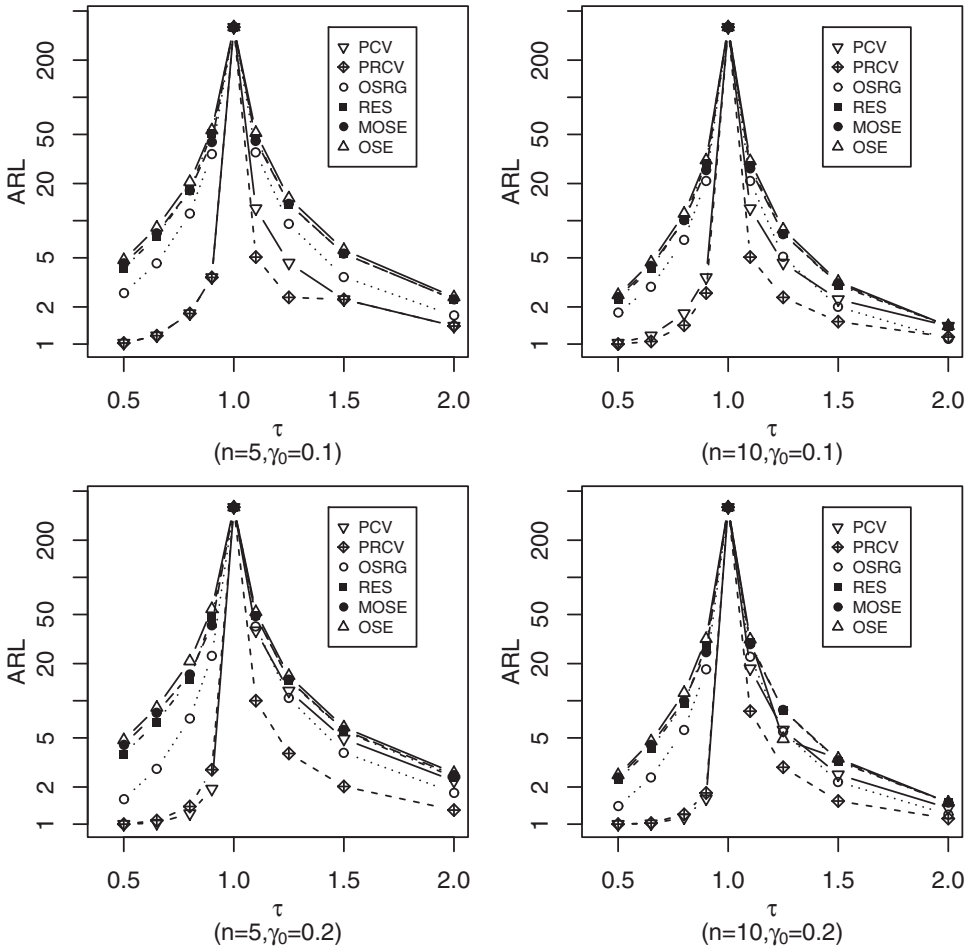

Figure 1 The ARL values and relative mean index values of the PCV, PRCV, OSRG, RES, MOSE, and OSE charts ($ARL_0 = 370$)

4 | COMPARISONS

In this section, the performances of the proposed schemes are compared with those of several memory-type CV schemes, namely, the OSRG,[13] RES,[12] OSE,[3] and MOSE[7] schemes, respectively. Here, each scheme is calibrated such that $ARL_0 \approx 370$. For simplicity, the values of ARL are calculated from at least 30,000 RL simulations. Moreover, for each given combination (γ_0, τ, n), we set the upper bound of any RL value to 10,000. The Fortran programs are coded for the simulations.

The proposed PCV and PRCV procedures (Equations 7– 14) are different from the other procedures. The PCV and PRCV schemes are based on the progressive average model, while the other procedures are based on the weighted moving-average scheme. The PCV and PRCV schemes are not affected by the parameter of the statistic. That is the PCV and PRCV statistics are only composed of the observations and do not contain auxiliary parameters. However, corresponding to the OSRG chart, the combination of the parameters (q, α) is set to be (0.95, 0.75), and the RES, OSE, and MOSE schemes with the optimal combinations of the parameters are used.

Table 9 shows the simulation results. From Table 9, regardless of the values of n and γ_0, the PCV and PRCV control charts outperform the other four competing charts for any given shift sizes τ. In addition, the performance of the PRCV scheme is more perfect than the PCV scheme, especially for monitoring upward shift. For instance, for $\gamma_0 = 0.1$, $n = 5$, $\tau = 1.1$, the $ARL_1 = 12.55$ in the PCV chart, which is nearly 65.04% less than $\text{ARL}_1 = 35.9$ for the OSRG chart, 73.01% less than 46.5 for the RES scheme, 71.80% less than 44.5 for the MOSE scheme, and 75.63% less than 51.5 for the OSE chart. The PRCV scheme is more sensitive than the PCV chart. In the same scenario, $ARL_1 = 5.07$ in the PRCV scheme, which is nearly 59.60% faster than the PCV scheme. It can be seen that the performance of the PRCV model is quite powerful.

Table 10 The data sets of elongation of the 154dtex/36f type of the nylon 6 yarn from the spinning process

Phase I				Phase II			
k	$\bar{X}_k$	S_k	$\hat{\gamma}_k$	k	$\bar{X}_k$	S_k	$\hat{\gamma}_k$
1	18.96	1.86	0.0981	1	17.34	2.10	0.1211
2	18.59	2.30	0.1237	2	20.18	1.98	0.0981
3	17.65	2.25	0.1275	3	19.66	2.11	0.1153
4	19.74	2.36	0.1196	4	19.73	2.32	0.1176
5	18.80	2.16	0.1179	5	21.08	2.75	0.1305
6	19.97	2.50	0.1252	6	17.89	2.26	0.1263
7	20.43	2.58	0.1263	7	19.67	1.91	0.0971
8	17.86	2.33	0.1305	8	18.49	2.38	0.1287
9	17.19	2.09	0.1216	9	17.69	2.31	0.1306
10	21.63	2.15	0.0994	10	17.72	2.33	0.1315
11	22.43	2.16	0.0963	11	18.01	2.47	0.1371
12	18.86	2.35	0.1246	12	19.61	2.75	0.1402
13	17.26	2.21	0.1280	13	19.16	2.55	0.1331
14	18.35	2.19	0.1193	14	19.42	2.68	0.1380
15	20.24	2.19	0.1082	15	18.21	2.36	0.1296
16	19.91	2.33	0.1160	16	18.61	2.82	0.1515
17	17.28	2.17	0.1256	17	18.79	2.57	0.1367
18	19.33	2.45	0.1267	18	16.71	2.52	0.1508
19	17.17	2.26	0.1316	19	20.74	2.74	0.1321
20	18.78	2.31	0.1230	20	18.25	2.37	0.1299

As the shift size turn larger, for example, $\tau = 1.25$, the advantage of the two progressive CV charts decreases. In this case, $ARL_1 = 4.55$ in the PCV scheme, which is approximately 51.60% less than 9.4 for the OSRG scheme, 66.54% less than 13.6 for the RES and MOSE charts, and 70.07% less than 15.2 for the OSE scheme. In this case of $\tau = 1.25$, ARL_1 is 2.39 in the PRCV scheme, which is 47.47% smaller than that of the PCV chart. It can be shown that the smaller the upper-sided shift size, the more significant the advantage of the two progressive-CV-type control charts. Moreover, the performance of the upward PRCV chart is the most outstanding.

For the downward schemes, when $\gamma_0 = 0.1$, $n = 5$, and $\tau = 0.5$, $\mathrm{ARL}_1 = 1.02$ in the PCV scheme, which is 44.86% less than the 1.85 of the OSRG chart, 77.83% less than the 4.6 of the MOSE chart, and 78.75% less than the 4.8 of the OSE chart. When the shift turns smaller, for example, $\tau = 0.9$, the PCV and PRCV charts become more sensitive. In this case, $ARL_1 = 3.47$ in the PCV chart, which is nearly 90.03% less than 34.8 for the OSRG scheme, 93.24% less than 51.3 for the RES scheme, 92.00% less than 43.4 for the MOSE scheme, and 93.59% less than 54.1 for the OSE scheme.

We compare several sensitive CV schemes above based on the ARL_1 values. In order to compare the performances of these schemes more intuitively, we use the line graph to present the simulation results in Figure 1. It can be obtained that the two progressive-CV-type schemes are more effective than competitive schemes. Moreover, we use the values of the relative mean index (RMI) to assess the overall performances of the schemes over a range of shifts.

$$RMI = \frac{1}{N}\sum_{i=1}^{N}\frac{ARL_{(\tau_i)} - MARL_{(\tau_i)}}{MARL_{(\tau_i)}},$$

where $ARL_{(\tau_i)}$ is the ARL_1 value of the given chart for detecting a shift τ_i, $MARL_{(\tau_i)}$ is the smallest ARL_1 value of all of the compared charts, and N is the total number of shifts considered. The smaller RMI is, the better the performance of the control scheme is. The values of RMI indicate the PCV and PRCV schemes outperform other schemes. Thus, the proposed schemes significantly improve sensitivity and efficiency for the detection of the process CV shifts.

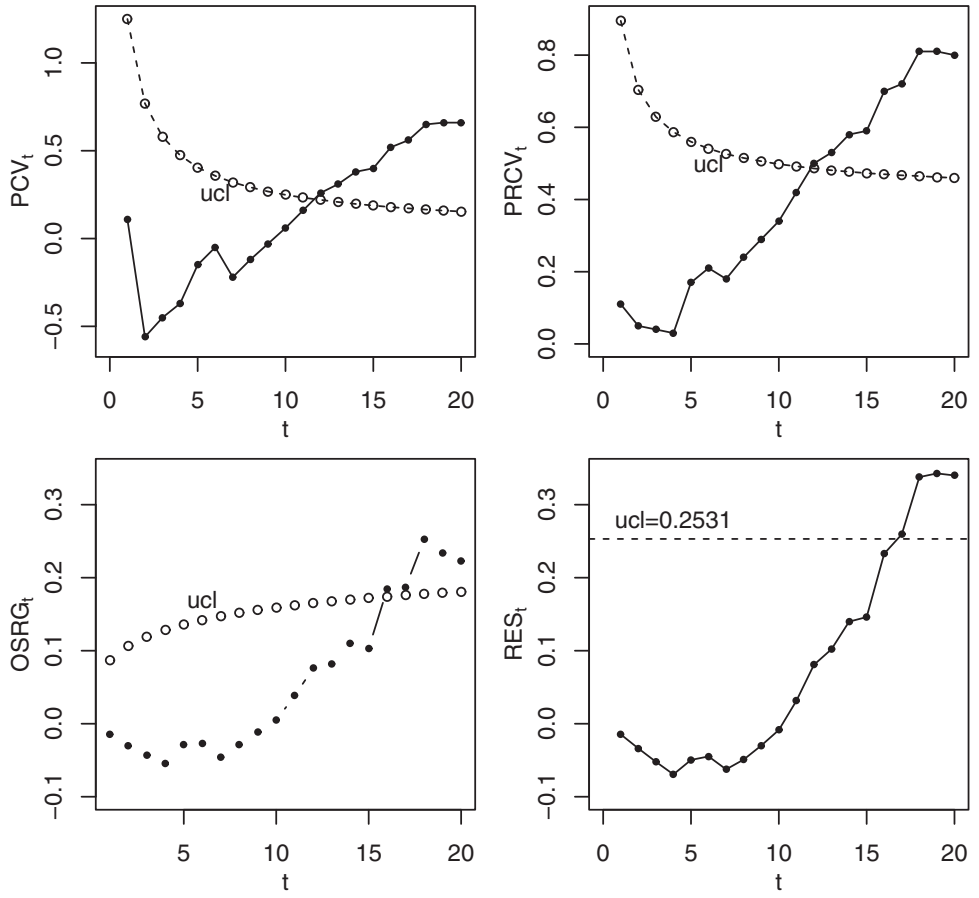

Figure 2 The PCV, PRCV, OSRG, and RES charts for monitoring the real data from a spinning process

5 | APPLICATIONS

We present the application to illustrate the proposed methodology through a numerical example from a spinning process in this section. We obtain the real data about the elongation of yarn from Chen et al.[13] The CV value of the elongation is related to the stability and reliability of the manufacturing processes and influences the grade of yarn. The elongations of yarn are shown in Table 10. The data set of 20 observations of size $n = 30$ on the elongation of the 154dtex/36f-type nylon 6 yarn is utilized for in control (Phase I) analysis. From the data set of Phase I, we can figure out the estimation of the IC CV value of elongation $\hat{\gamma}_0 = \frac{1}{20}\sum_{k=1}^{20} = 0.1195$. The upper-sided CV shifts are the monitored objective because the CV value of the elongation will be greatly increased when the other process parameters are OC, for instance the mean of the elongation decreases or the standard deviation increases.

The charting constant L^+ in the PCV chart is 1.258, while L^+ is 0.85 in the PRCV chart when $ARL_0 = 370$ through the search algorithm mentioned in Section 3.1. The 20 samples of size 30 are collected during Phase II. As a comparison, the parameter combination of the upward OSRG[13] scheme is set to $(q = 0.95, \alpha = 0.8, L^+ = 2.972)$. The optimal parameter combination $(K^* = 2.707, \lambda^* = 0.05)$ is used in the upward RES[12] scheme with the limit $UCL = 0.2531$.

The statistics and control limits of four compared upward schemes are presented in Figure 2. To detect the CV shift of the elongation of yarn, an OC signal is given at the 12th observation point in the PCV scheme. Similarly, the first OC sample is also the 12th point in the PRCV scheme. We can see that the OC signal is first triggered at the 16th point in the OSRG scheme, which is 4 runs later than that from the PCV and PRCV charts. While the RES chart detects the first OC signal is at the 18th samples, which is 5 runs later than that from the PCV and PRCV charts. We find the value of the 12th sample 0.1402 is greater than several values adjacent to each other. And the value of the 12th sample is 17.32% greater than the IC value of 0.1195. Thus the 12th sample is an obvious precursor of upward shift, which is not triggered by the OSRG and RES charts. The first OC signal is shown ever later at the 17th point in the OSE[3] and MOSE[7] schemes by calculation. So the PCV and PRCV schemes are more sensitive than the other completing charts for detecting CV shifts.

6 | SUMMARY

We present two progressive average type schemes to detect CV process shifts, which are PCV and PRCV charts. Based on the numerical results, the overall conclusion is that the two proposed control charts are superior to all the compared other memory-type charts. The advantages of the two proposed progressive-CV-type charts are greater as the shift sizes are smaller. Especially, the performance of the PRCV chart is the most outstanding in all existing CV control charts for the upward CV shifts which are often monitored in practice.

The proposed schemes significantly improve the sensitivity for monitoring the CV shifts. To sum up, the progressive-CV-type schemes have the following advantages. First, because the PCV and PRCV schemes use the adjusted time-varying control limits, the detection ability of the proposed schemes is obviously better than other control charts with the fixed control limits, in detecting start-up problems and small shifts. Second, the two proposed schemes are easily operated in application because they need no additional parameters in the monitored statistics except for the control limit constant L, which is not affected by the magnitude of the shift. Third, the improvement of the PRCV scheme in monitoring efficiency largely depends on the appliance of resetting technique to overcome the inertia problem. In summary, the two proposed progressive-CV-type schemes offer simple, handy, and efficient tools for practitioners to minor various kinds of CV shifts. In the future, researchers can extend the CV chart to the nonparametric field, which is our next research direction.

ACKNOWLEDGMENTS

The authors are thankful to the anonymous reviewer for the valuable and constructive comments that have vastly improved this paper. This paper is supported by the Project of Hebei Educational Department of China (No. GH201007 and No. 2018GJJG177), the General Program of Natural Science Foundation of Hebei Province (No. A2019207064), the National Natural Science Foundation of China (No. 12071233), the General Program of Natural Science Foundation of Liaoning Province (No. 2020-MS-139), the Project of Science and Research of Liaoning Educational Department of China (No. LJC202006), the Program of Natural Science Foundation of Liaoning Province (No. 2019ZD-0193), the Project of Science and Research of Hebei Educational Department of China (No. ZD2019073 and No. QN2017328), the Science and Technology Project of Hebei Science and Technology Department of China (No. 162176489), and the Project of Science and Research of Hebei University of Economics and Business (No. 2018ZD06 and No. 2017KYQ09).

ORCID

Rui Chen https://orcid.org/0000-0003-4629-9733
Li Jin https://orcid.org/0000-0003-4122-4943
Zhonghua Li https://orcid.org/0000-0002-0927-226X

REFERENCES

1. Kang CW, Lee MS, Seong YJ, Hawkins DM. A control chart for the coefficient of variation. *J Qual Technol*. 2007;39:151-158.
2. Hong E, Kang C, Baek J, Kang H. Development of CV control chart using EWMA technique. *J Soc Korea Ind Syst Eng*. 2008;31:114-120.
3. Castagliola P, Celano G, Psarakis S. Monitoring the coefficient of variation using EWMA charts. *J Qual Technol*. 2011;43:249-265.
4. Calzada ME, Scariano SM. A synthetic control chart for the coefficient of variation. *J Stat Comput Simul*. 2013;83:853-867.
5. Castagliola P, Achouri A, Taleb H, Celano G, Psarakis S. Monitoring the coefficient of variation using a variable sampling interval control chart. *Qual Reliab Eng Int*. 2013;29:1135-1149.
6. Castagliola P, Achouri A, Taleb H, Celano G, Psarakis S. Monitoring the coefficient of variation using control charts with run rules. *Qual Technol Quant Manag*. 2013;10:75-94.
7. Zhang J, Li Z, Chen B, Wang Z. A new exponentially weighted moving average control chart for monitoring the coefficient of variation. *Comput Ind Eng*. 2014;78:205-212.
8. Castagliola P, Amdouni A, Taleb H, Celano G. One-sided Shewhart-type charts for monitoring the coefficient of variation in short production runs. *Qual Technol Quant Manage*. 2015;12:53-67.
9. Amdouni A, Castagliola P, Taleb H, Celano G. Monitoring the coefficient of variation using a variable sample size control chart in short production runs. *Int J Adv Manuf Technol*. 2015;81:1-14.
10. Li Z, Qiu P. Statistical process control using a dynamic sampling scheme. *Technometrics*. 2014;56:325-335.
11. You HW, Khoo MB, Castagliola P, Haq A. Monitoring the coefficient of variation using the side sensitive group runs chart. *Qual Reliab Eng Int*. 2016;32:1913-1927.
12. Zhang J, Li Z, Wang Z. Control chart for monitoring the coefficient of variation with an exponentially weighted moving average procedure. *Qual Reliab Eng Int*. 2018;34:188-202.
13. Chen R, Li Z, Zhang J. A Generally weighted moving average control chart for monitoring the coefficient of variation. *Appl Math Model*. 2019;70:190-205.

14. Abbasi SA, Abbas T, Adegoke NA. Efficient CV control charts based on ranked set sampling. *IEEE Access*. 2019;7: 78050-78062.
15. Abbasi SA. Efficient control charts for monitoring process CV using auxiliary information. *IEEE Access*. 2020;8: 46176-46192.
16. Agarwal BL. *Programmed Statistics*. 2nd edition. New Delhi: New Age International Publishers; 2003.
17. Abbas N, Zafar RF, Riaz M, Hussain Z. Progressive mean control chart for monitoring process location parameter. *Qual Reliab Eng Int*. 2013;29(3):357-367.
18. Abbasi SA, Miller A, Riaz M. Nonparametric progressive mean control chart for monitoring process target. *Qual Reliab Eng Int*. 2013;29(7):1069-1080.
19. Zafar RF, Abbas N, Riaz M, Hussain Z. Progressive variance control charts for monitoring process dispersion. *Commun Stat Theory Methods*. 2014;43(23):4893-4907.
20. Abbas N. Progressive mean as a special case of exponentially weighted moving average. *Qual Reliab Eng Int*. 2015;31(4):719-720.
21. Abbasi A. Poisson progressive mean control chart. *Qual Reliab Eng Int*. 2017;33(8):1855-1859.
22. Zafar RF, Mahmood T, Abbas N, Riaz M, Hussain Z. A progressive approach to joint monitoring of process parameters. *Comput Ind Eng*. 2018;115:253-268.
23. Abbas Z, Nazir HZ, Akhtar N, Riaz M, Abid M. An enhanced approach for the progressive mean control charts. *Qual Reliab Eng Int*. 2019;35(4):1046-1060.
24. Alevizakos V, Koukouvinos C. A progressive mean control chart for monitoring time between events. *Qual Reliab Eng Int*. 2020;36:161-186.
25. Shu L, Jiang W. A new EWMA chart for monitoring process dispersion. *J Qual Technol*. 2008;40:319-331.
26. Iglewicz B, Myers R, Howe RB. On the percentage points of the sample coefficient of variation. *Biometrika*. 1999;55:580-581.
27. Breunig R. An almost unbiased estimator of the coefficient of variation. *Econ Lett*. 2001;70:15-19.
28. Barr DR, Sherrill ET. Mean and variance of truncated normal distributions. *Am Stat*. 1999;53:357-361.
29. Qiu P. *Introduction to Statistical Process Control*. 1st edition. Boca Raton FL: Chapman and Hall/CRC; 2014;:169-173.
30. Li Z, Zou C, Gong Z, Wang Z. The computation of average run length and average time to signal: an overview. *J Stat Comput Simul*. 2014;84:1779-1802.

How to cite this article: Chen R, Jin L, Li Z, Zhang J. A progressive approach for the detection of the coefficient of variation. *Qual Reliab Eng Int*. 2021;37:2587–2602. https://doi.org/10.1002/qre.2877